Refractive index of ionic liquids under electric field: Methyl propyl imidazole iodide and several derivatives*

Ji Zhou(周吉)[1], Shi-Kui Dong(董士奎)[2], Zhi-Hong He(贺志宏)[2], and Yan-Hu Zhang(张彦虎)[3,†]

[1] *Beijing Institute of Space Mechanics & Electricity, Beijing* 100094, *China*
[2] *School of Energy Science and Engineering, Harbin Institute of Technology, Harbin* 150001, *China*
[3] *Advanced Manufacturing & Equipment Institute, Jiangsu University, Zhenjiang* 212013, *China*

(Received 10 November 2019; revised manuscript received 8 February 2020; accepted manuscript online 13 February 2020)

Ionic liquids have received wide attention due to their novel optoelectronic structures and devices as an optical means of regulating electricity. However, the quantitative testing and analysis of refractive index of ionic liquids under electric field are rarely carried out. In the present study, an experimental apparatus including a hollow prism is designed to measure the refractive indices of ionic liquids under different electric fields. Five groups of imidazole ionic liquids are experimentally investigated and an inversion is performed to determine the refractive indices under electric fields. The error propagation analysis of the apex angle and the minimum deflection angle are conducted, and the machining accuracy requirements of the hollow prism are determined. The results show that the refractive indices of imidazole ionic liquids change with the light wavelength, following a downward convex parabola. Furthermore, the refractive index decreases with the carbon chain length of ionic liquid at a given wavelength, presenting an order of C_3MImI > C_4MImI > C_5MImI > C_3MImBr > C_3MImBF_4. Notably, the refractive index of imidazole ionic liquid exhibits a nonlinear change with the applied voltage at 546 nm and a monotonical decrease at 1529 nm. Besides, the variation of refractive index at 1529 nm with the applied voltage is larger than that at 546 nm and 1013 nm. Importantly, the variation of refractive index is contrary to that of absorption coefficient under electric field. This study illustrates that the theory of electrode and carrier transport can be used to explain the law of variation of *n*–*k* value of ionic liquid under the electric field, and provides the support for the evaluation of physical properties of ionic liquids, the measurement of optical functional parameters and the regulation of electric–optic performances of optical devices.

Keywords: ionic liquid, refractive index, electro–optical property, uncertainty propagation analysis

PACS: 78.20.Ci, 78.30.cd, 78.20.Jq, 33.57.+c **DOI:** 10.1088/1674-1056/ab75cd

1. Introduction

Room-temperature ionic liquids or simply ionic liquids (ILs) are of great interest because of their excellent electric, magnetic, acoustic, thermal, and optical properties.[1–3] For instance, various superconducting materials consisting of ionic liquids and hard materials are useful for unique electro–optical,[4] magneto–optical,[5] and/or thermo–optical properties,[6] resulting in an important viewpoint that ionic liquids are marked as one of promising functional materials in 21st century.[7] The light–matter interaction represents the composite of the electric and magnetic responses of IL material, which can be quantified by a single parameter called the complex refractive index (CRI).[8] Complex refractive index is the most important optical constant of absorptive medium, which is determined by the dielectric coefficient of materials.[9] The refractive index and absorption coefficient correspond to the real part and the imaginary part of the complex refractive index of the absorbing material, respectively. As shown by Wang *et al.*,[10] ionic liquids can be used for electrically controlling optical media and implementing the electro–optical control in a wide spectral range. In our previous study,[11] we found that the absorption coefficient of the imidazole ring increases with voltage increasing in a spectral range from 1520 mm to 1960 mm. The variation range is affected by the length of carbon chain and the type of anion on the imidazole ring. As is well known, the refractive index is of interest for substance identifying, purity checking, and concentration measuring.[12] Given that the electric field availably affects the absorption coefficient of the ionic liquid at a specific wavelength, it is speculated that the electric field will influence the refractive index of the ionic liquid at the specific wavelength.

There are many studies focusing on the calculation and prediction of physical properties of ionic liquids. For instance, the refractive index of the mixed solution of 1-alkyl 3-methyl imidazole 4-fluorborate and water and ethanol were predicted by Newton model and Gladstone-Dale model.[13] Wang *et al.*[14] predicted the refractive indioces of IL at different temperatures from 283.15 K to 368.15 K by using group contribution-artificial neural network model and group contri-

*Project supported by the National Natural Science Foundation of China (Grant Nos. 51576054 and 51705210) and the Jiangsu Provincial Planned Projects for Postdoctoral Research Funds, China (Grant No. 2019K195).

†Corresponding author. E-mail: zhyh@ujs.edu.cn

© 2020 Chinese Physical Society and IOP Publishing Ltd

bution method. The results showed that the average absolute relative deviations of the former model and the latter method are 0.179% and 0.628%, respectively. Kang *et al.*[15] predicted the refractive index of ionic liquid from molecular descriptor calculated by the quantum chemistry method through using the extreme learning machine intelligence algorithm and a multiple linear regression approach. Allan *et al.*[16] presented a model for predicting the refractive index of binary ionic liquid system containing alcohol by using the artificial neural network algorithm. The refractive index was correlated with temperature, mole fraction, the number of carbon atoms in the cation, the number of carbon atoms in the anion, the number of hydrogen atoms in the anion, and the number of carbon atoms in the alcohol. Eva *et al.*[17] found that the refractive index linearly decreases with temperature rising. The refractive indices of the mixtures of the 1-ethyl-3-methylimidazolium acetate with methyldiethanolamine increased with the mole fraction increasing and decreased with temperature rising.[18] However, these theoretical estimation methods encounter insurmountable difficulties and are hard to assess their original attractiveness under complex multi-physics fields.

Furthermore, ionic liquids have good optical–electrical properties, which also give higher possibilities toregulate the refractive index of ionic liquids, especially in the application fields of temperature, electric field and magnetic field coupling. Therefore, the intrinsic relationship between refractive index and other physical parameters have received extensive attention. This research trend arises from great expectations for the measurement method and accurate results of refractive index. The refractive indices of 1-ethyl-3-methylimidazolium tetracyanoborate in a temperature range of 283.15 K–313.15 K were obtained by using an Abbe measuring instrument.[19] Bhattacharjee *et al.*[20,21] measured the refractive index of phosphonium based/ sulfonium- and ammonium-based ionic liquids by using an automated refractometer at the atmosphere. The results showed that the maximum temperature deviation is 0.01 K, whereas the maximum uncertainty of the refractive index measurements is 0.0005. The refractive indices of 17 kinds of room-temperature ionic liquids at different temperatures were measured by Seki *et al.*,[22] and showed that the electron polarization of ionic liquid mainly contributes to the refractive index of ionic liquid, and there is a high linear correlation between polarization and refractive index. Xu *et al.*[23] measured the surface tensions, densities and refractive indices of amino acid ionic liquids at different temperatures. Wang *et al.*[10] found that the refractive index of the ionic liquid increases with the chain length of the cation increasing. The refractive index of the ionic liquid decreases with the anion size and the external temperature increasing, and has a linear relationship with the chain length of the cation when the anion is constant. In addition, difference between the physical properties of ionic liquids and their derivatives has become an interesting issue. As is well known, the ion cage structure plays an essential role in determining the structural and dynamic properties of the iconic liquids.[24] For instance, the density and the refractive index of the ionic liquid 1-alkyl-3-methylimidazolium cation with a chloride anion decrease with the alkyl side chain length in the cation increasing as temperature rises from 288.15 K to 318.15 K.[25] Montalbán *et al.*[26] found that the refractive index of 1-alkyl-3-methylimidazolium-based ionic liquid increases with alkyl chain length of cations increasing.

Hitherto, many efforts have been devoted to the study on the refractive index of ionic liquid theoretically and experimentally. However, little is known about the refractive index measurements and light refractive behaviours of ILs under electric field. Considering the fact that the electric field affects the absorption coefficient of imidazole IL, this result urges us to explore the effect of electric field on the refractive index of imidazole IL. Obviously, the influence of the electric field on the refractive index is helpful for us to master comprehensively the specific change law of the dielectric properties of the ionic liquid under the electric field. Moreover, the knowledge of the electro–optic properties of ionic liquids under an applied electric field is limited. For their optical parameters in an electrical field, it is hardly possible to quantitatively identify the effect of the types of cations and anions and carbon chain length on the optical properties of ionic liquids on their refractive index. Such a predicament prevents ionic liquids from being further developed and put into practical application. In addition, considering that the dielectric properties are affected by the temperature field, it is necessary to ascertain the variation rule of the dielectric properties under the electric field. This work will provide a theoretical foundation for regulating the thermo–optic behaviors of iconic liquids through the electro–optic effects.

2. Experiment

2.1. Materials

The materials used in this study were C_3MImI and its four derivatives including methyl butyl imidazole iodide (C_4MImI), methyl pentyl imidazole iodide (C_5MImI), methyl propyl imidazole bromide (C_3MImBr), and methyl propyl imidazole tetrafluoroborate (C_3MImBF_4) as shown in Table 1. All the ionic liquids (purity better than 99.5%) were purchased from the Lanzhou Institute of Physical Chemistry, Chinese Academy of Sciences.

Table 1. Molecular structures of iconic liquid C_3MImI and four derivatives.

Ionic liquid	Molecular structure	Anion substituent	Carbon chain length
C_3MImI	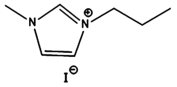	I	3
C_4MImI	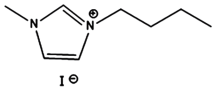	I	4
C_5MImI	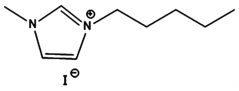	I	5
C_3MImBr	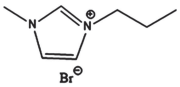	Br	3
C_3MImBF$_4$	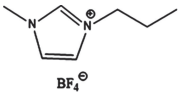	BF_4	3

2.2. Apparatus and methods

The experiment was based on the high precision refractive index measurement system at the Crystal Research Center of the Institute of Physics and Chemistry, Chinese Academy of Sciences. The original device was used to measure the refractive index of the translucent crystal through using the minimum deflection angle method. Its core equipment was SpectroMaster, a fully automatic high precision refractive index measuring instrument. The platform was composed of a light source (lamp), collimator, goniometer/detector, phase locked amplifier, chopper, chopper power supply, infrared detector power, PMT power supply, lamp, signal generator, and mobile and rotating samples. The wavelengths available were 546 nm, 587 nm, 706 nm, 852 nm, 1013 nm, 1529 nm, and other specific bands of its own light source. The measurement principle of refractive index of ionic liquid is shown in Fig. 1. The refractive index is calculated from formula (1) by measuring the top angle of crystal prism and the minimum deflection angle of light transmission,

$$n = \frac{\sin\left(\delta_{\min} + A\right)/2}{\sin\left(A/2\right)}. \tag{1}$$

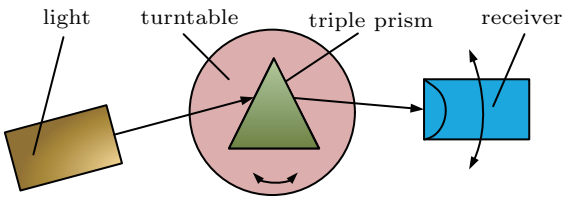

Fig. 1. Measurement principle of refractive index of ionic liquid.

To measure the refractive index of ionic liquid under the applied electric field, a special hollow prism was designed and manufactured. A voltage-adjustable direct current (DC) power supply was added to meet the requirements for measuring the refractive indices of soft liquid electro–optic materials under an applied electric field. The hollow prism was a key to the high-precision measurement of the refractive index. The requirements in three aspects related to the measuring errors needed to be meet. Firstly, the refractive index of soft liquid electro–optic material is available under an electric field. Secondly, the hollow prism used in the method of minimum deflection angle for loading liquid meets the requirements of high-precision processing. Thirdly, the structure and material selection of the test piece meet the requirements of visible-infrared multi-spectral band measurement. The most difficult problem is the machining accuracy. It is necessary to ensure that the measurement error of the minimum deviation angle and the sample top angle meet the above-mentioned conditions.

According to the manual of SpectroMaster measuring instrument, the absolute refractive index measuring error of the system can reach 10^{-6}. In order to achieve this level resolution, three conditions are necessary and shown as follows: the fabrication accuracy of the prism is better than that of the $\lambda/10$ (PV at 632.8 nm), the measuring error of the apex angle A is less than 0.2 arcsec, and the measuring error of the minimum deflection angle is less than 0.4 arcsec.

According to the above requirements, the final design of the hollow prism for the liquid to be tested is shown in Fig. 2, where three equally thick quartz glasses and two platinum plated platinum electrodes are located on the top and bottom, respectively. In order to reduce the multiple reflections, refractions and diffraction phenomena and enhance the signals collected in the detector, the inner and outer surfaces of the third glass and the bonding edges of the three glass were textured. The diaphragm, parallelism, surface precision, optical path distance of the two pieces of glass and the tower difference of the whole piece are of high precision. The parallelism of the two pieces of glass is controlled within $3''$, the tower

difference is within 1′ after being wholly glued, and the two pieces of glasses are equal in optical path, the optical path error is less than 0.1λ. Finishing surface is perpendicular to the upper and lower bottom surface, requiring that the root-mean-square (RMS) values of the crests and troughs of the convex surface should be less than 1/10 wavelength. The platinum electrode was connected to the voltage adjustable DC power supply to realize the regulation of external electric field.

The test system of refractive index for iconic liquids under an applied voltage is shown in Fig. 3, where the light source part was composed of various spectral lights 1, tower 2, mirror 3, light power supply 4, condenser 5, chopper 6, chopper controller 7, color filter converter 8, and adjustable slit 9. The light was collimated through a collimator 10. The detector and signal receiving part were composed of telescope 15, infrared detector 16, photomultiplier 17, lock-in amplifier controller 18, lock-in amplifier 19, and CCD camera 20. The tested sample 22 was placed on a piezoelectric drive platform 12, and the drive platform was set on a tray balance 13 which was located on a pneumatic bearing bracket 14. The power was provided by a voltage adjustable DC power supply. The measuring experiments were conducted at room temperature (22 ℃) and atmosphere pressure.

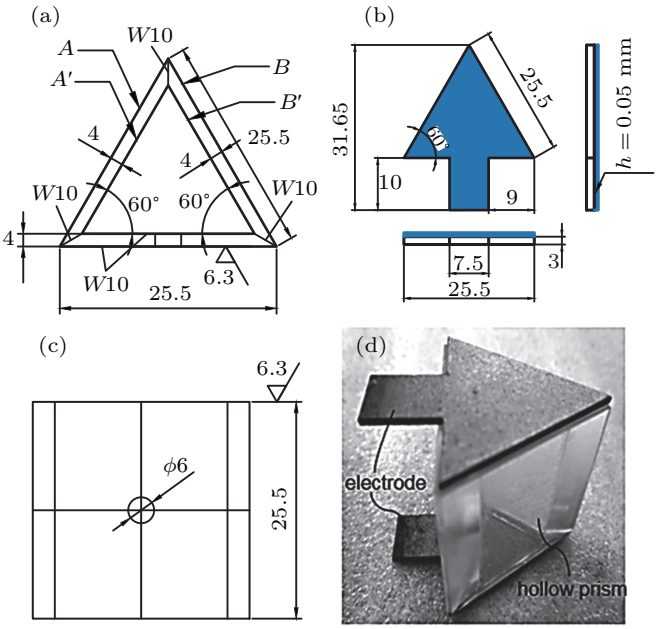

Fig. 2. Geometric dimensions and physical photos of hollow prism.

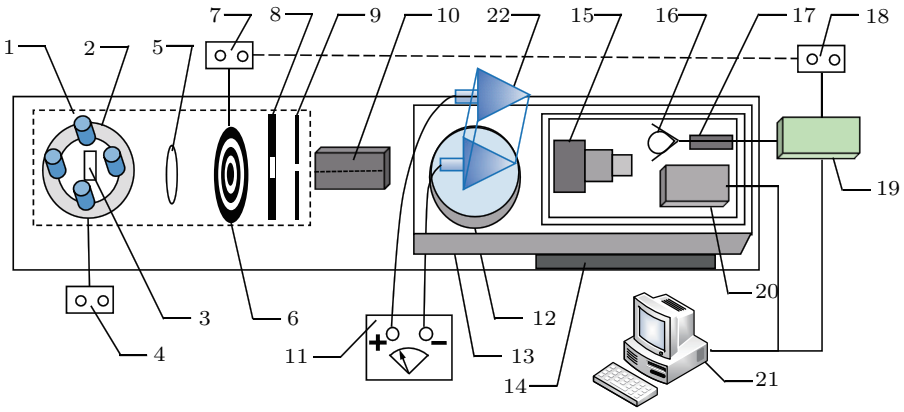

Fig. 3. Ionic liquid refractive index measuring system and its composition.

2.3. Measuring error analysis

2.3.1. Error sources

Before the test, the top angle of hollow prism was measured repeatedly. In this paper, the top angle of prism was 59.99114°. In the process of measuring the minimum deviation angle, the value was kept unchanged. In addition, the accuracy of the experimental platform was verified by measuring the refractive index of cure water prepared by Millipore Elix pure water system. Five groups of pure water measurement experiments were carried out by using a 587.65-nm light source at an atmospheric pressure and a temperature of 22 ℃, and the measured results were 1.3327272, 1.3227278, 1.3327274, 1.3327276, and 1.3327275, respectively. The relative deviation between the measurement results and the values reported in Ref. [27] is about 6.2×10^{-5}.

From the measurement method, the error of the refractive index measurement system is mainly composed of two parts, *i.e.*, apex angle error and minimum deflection angle error (see Fig. 4). For the apex angle of the hollow prism, the error is not only related to the system angle measurement error, but also has a direct relationship with the non-parallelism of the inner and outer surfaces of the glass. Thus, the total error of the apex angle is the accumulate error of the above two aspects of errors. The system error of the measurement angle was less than 0.036 arcsec (0.00057312°), and the non-parallelism of the left and right glass was controlled within 3″. Therefore, the total error of the apex angle introduced by the entire prism to be tested was no more than 6″. The total angle error of the apex angle was the sum of the error caused by the systematic error and the non-parallelism, which was 0.0378 arcsec. Therefore,

the apex angle error of the experimental sample in this paper met the technical requirements (less than 0.2 arcsec).

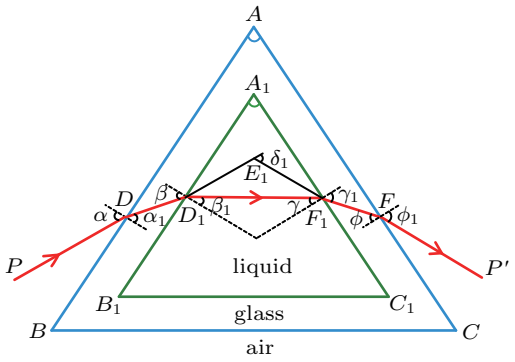

Fig. 4. Physical model of hollow prism by using minimum deviation angle method.

2.3.2. Error propagation analysis

Preliminary experiments have shown that the tower difference increases when the height/side length ratio is too large. When the height/side length ratio is too small, the prism surface deformation is usually caused by the three-side bonding, which affects the overall aperture accuracy. Therefore, it is necessary to process the three sides of the prism in an equilateral triangle and keep the ratio of height/side length within an appropriate range. A small hole was opened on one side of the hollow prism for injecting and withdrawing the liquid to be tested. The actual hole was blocked by using a rubber stopper to prevent the liquid from leaking. An error model of minimum deviation angle is established (see Fig. 5), and then the necessary machining accuracies for the hollow prism assemblies are obtained. The detailed derivation process is presented in supporting information (S1. Error model analysis in measuring liquid minimum deviation angle by considering the influence of the nonparallelism).

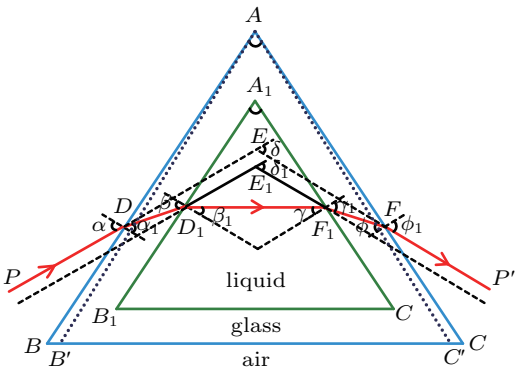

Fig. 5. Error model of minimum deviation angle with effect of non-parallelism.

The refractive indices, the exit angle of the glass–liquid interface β_1, the incident angle of the glass–liquid interface γ, and the maximum nonparallelism error of the prism caused by machining $\Delta\theta_3$ are related as follows:

$$\arcsin\left(\frac{n_{\text{liquid}}\sin\beta_1}{n_{\text{glass}}}\right)=\Delta\theta_3+\arcsin\left(\frac{n_{\text{liquid}}\sin\gamma}{n_{\text{glass}}}\right). \quad (2)$$

In the above derivation process of Eq. (2), it was considered that the size of liquid prism does not change, so the following still hold true:

$$\beta_1+\gamma=\angle A_1, \quad (3)$$

$$\beta_2=\arcsin\left(n_{\text{liquid}}\cdot\sin\beta_1\right), \quad (4)$$

$$\gamma_2=\arcsin\left(n_{\text{liquid}}\cdot\sin\gamma\right), \quad (5)$$

$$\Delta\beta_1=\Delta\gamma=\Delta A_1, \quad (6)$$

$$\Delta\beta_2=\frac{1}{\sqrt{1-n_{\text{liquid}}^2\sin^2\beta_1}}\cdot n\cdot\cos\beta_1\cdot\Delta\beta_1, \quad (7)$$

$$\Delta\gamma_2=\frac{1}{\sqrt{1-n_{\text{liquid}}^2\sin^2\gamma}}\cdot n\cdot\cos\gamma\cdot\Delta\gamma, \quad (8)$$

$$\Delta\delta_1=|\Delta\beta_2|+|\Delta\gamma_2|+|\Delta A_1|. \quad (9)$$

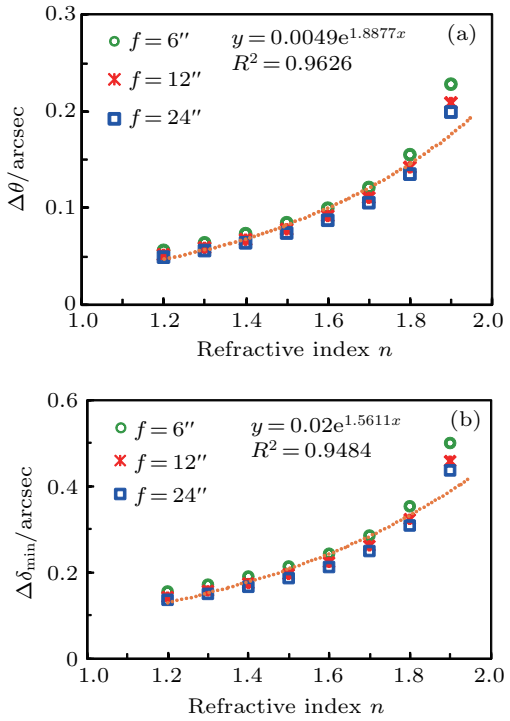

Fig. 6. (a) Error between (a) incident/departure angle and ideal angle of the liquid three prism and (b) error analysis of minimum deviation angle considering the influence of the non-parallelism.

The total error of the final minimum deflection angle is composed of the following three items. Figure 6(a) shows the refractive index of the glass at 1.459 (corresponding to wavelength 546 nm) and 1.444 (corresponding to wavelength 1530 nm), according to Eqs. (7) and (8). The calculated maximum absolute error of the incident angle and the exit angle of the liquid triangular prism with respect to the incident angle and the exit angle is a function of the true refractive index of the liquid. Figure 6(b) shows the relationship between the maximum absolute error of the minimum deflection angle calculated according to Eq. (9) and the true refractive index of the liquid when the minimum glass refractive indices are 1.459 and 1.444, respectively. It can be seen that the above absolute error gradually increases with the true refractive index of the

liquid increasing, but it is not affected by the refractive index of the glass in a range from 500 nm to 2000 nm. In addition, for the case where the overall non-parallelism is $6''$, it can be seen that the absolute error of the minimum deflection angle is less than 0.4 arcsec when the liquid refractive index is less than 1.86. The error analysis of the above apex angle can be obtained for the experimental device. Then, a measurement accuracy of 10^{-6} can be achieved when the liquid refractive index is less than 1.86.

2.3.3. Machining accuracy

Based on the above analysis, the glass was processed and adhered by using glass glue, and the flowchart is shown in Fig. 7. According to the design requirements, the substrate was cut into a cuboid with 1 mm in length, 1 nm in width, and 0.2 mm in thickness. The side of the glass piece was roughly ground so that the angular accuracy was $\pm 4^{\circ}$. Side polishing with a four-axis machine achieved a smooth finish of grand three, an aperture of three, and a parallelism of $15''$. The machining accuracy of this part is required to be extremely high, and the ultra-precision continuous polishing process was adopted for a higher measurement accuracy and reliability. Fine polishing was performed after rough polishing. The aperture was adjusted to one circle by regulating the calibration plate so that its parallelism was $5''$ and its finish reached grade two. Since this component was used to measure the refractive index, it was necessary to repair the optical path to make the light propagate well along it. The processed surface finish reached $1/60\lambda$ and passed the test to confirm whether the measurement requirements were satisfied. In the process of polishing, ZDHP-30 interferometer was used for monoitoring the test process. For the high angle requirement of this piece, when the optical cold glue is glued, the collimation angle is adjusted to meet the design requirements through using the parallel light pipe.

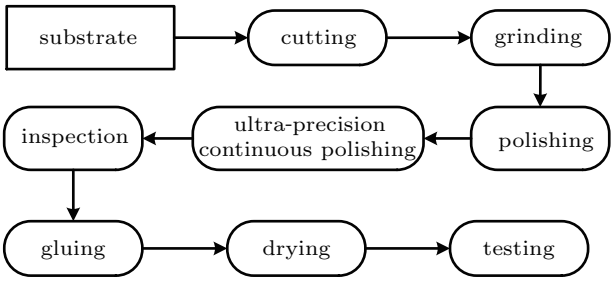

Fig. 7. Machining processing flowchart of glass plates for hollow prism.

2.4. Measuring procedure

Prior to the test, the inner and outer surface of the hollow prism were cleaned with alcohol, followed by wiping it with the cotton swab and keeping it clean (Because the actual light-passing surface is limited, the edge of the cotton swab cannot be wiped, but no other liquid remains), and drying it in a constant temperature oven (usually for 24 h). Prior to testing it, the hollow prism was taken out from the drying box. For the sample of the hollow prism of the ionic liquid to be tested, it was ensured that the orifice was placed vertically upward when the liquid was injected, and that the sample stood up for a while until the bubble overflows. For the center or the edge, the small bubble movable test piece caused the small bubbles to gather into a large bubble and then were sucked out by the syringe needle. After the liquid was filled in the entire liquid cavity, the outlet was sealed with a rubber plug to prevent the liquid from overflowing, and the conductive metal piece of the upper end and the lower end of the hollow prism were clamped by the electrode holder. In order to reduce the resistance, several silver-plated wires were used for the power supply line, and a thinner wire was selected to avoid the wire covering the light-passing hole of the detector due to improper operation during the test. The wire resistance was less than 0.05 Ω and the resistance difference between the two wires was less than 0.005 Ω. The two ends of the sandwiched prism were connected to the positive and negative pole of the power supply, respectively. The entire sample was placed on the sample stage on the automatic high-precision refractive index measuring instrument, the sample was screwed to the moving platform with a mechanical mold of the same size as the sample, or it was stuck with a sticky substance, to prevent the relative position of the sample and the turntable from moving when the turntable moved. According to the minimum deflection angle method, the refractive indices of the ionic liquids at different wavelengths were accurately measured under the applied electric field.

3. Results and discussion

3.1. Effects of wavelength

After the preparation of the test piece and the calibration of the test system, we firstly measure the refractive indices of five kinds of iconic liquids (*i.e.*, C_3MImI, C_4MImI, C_5MImI, C_3MImBr, C_3MImBF_4) under no action of external electric field at the wavelengths of 546 nm, 706 nm, 852 nm, 1013 nm, 1529 nm.

The influence of an electric field on the ionic liquid refractive index for wavelengths of 546 nm, 1013 nm, 1529 nm are investigated. The voltages 0 V, 0.5 V, 1 V, 1.5 V (due to the electrode spacing of 2.5 cm, if the voltage is raised to 2 V, the ionic liquid may be decomposed and ionized) are applied one by one in sequence. The method of repeated measurement is adopted, and the number of repeated measurements for each experimental group of data is not less than five.

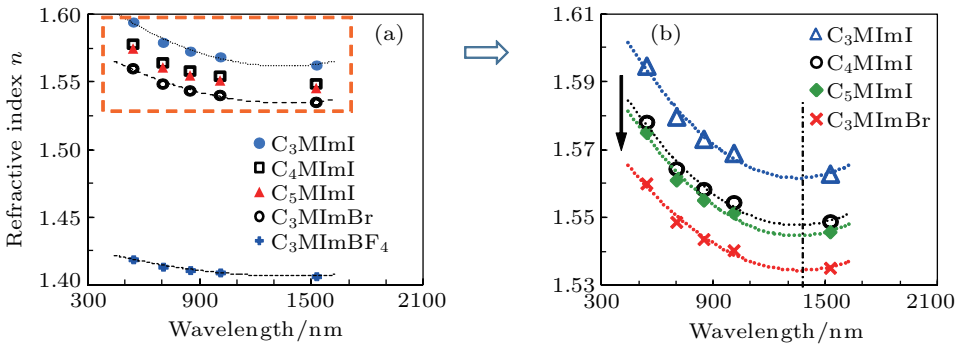

Fig. 8. Variations of refractive index of imidazole ionic liquids with wavelength.

The refractive indices of the five ionic liquids changing with the light wavelength are shown in Fig. 8. As can be seen, the refractive indices of these ionic liquids decrease with the wavelength increasing, and the refractive indices of these ionic liquids are ordered as follows: C_3MImI > C_4MImI > C_5MImI > C_3MImBr > C_3MImBF$_4$. Note that when ehancing the number of carbon atoms of the imidazole ring to increase and branch anion and cation binding capacity (bond energy), the refractive index of the ionic liquid exhibits a global decrease. The main reason is that a stronger hydrogen bond IL results in a higher refractive index. In addition, the anionic change will result in a greater refractive index of IL than that of cationic. Meanwhile, of the aforementioned ILs, the variation of the refractive index of C_5MImI with wavelength is the most obvious and that of the C_3MImBF$_4$ is little. Furthermore, for the methyl propyl imidazole iodide and several derivatives, a uniform relation between the refractive index and the light wavelength can be obtained by data fitting as expressed by Eq. (10).

$$n = C_0 - C_1\lambda + C_2\lambda^2. \tag{10}$$

For the five ionic liquids, the fitting coefficients are listed in Table 2.

Table 2. Fitting coefficients of relation between the refractive index and wavelength.

Coefficient	C_3MImI	C_4MImI	C_5MImI	C_3MImBr	C_3MImBF$_4$
C_0	1.6509	1.6298	1.6267	1.60256	1.4399
$C_1(\times10^{-4})$	1.3212	1.2147	1.2166	0.9962	0.4800
$C_2(\times10^{-8})$	4.8903	4.4928	4.5094	3.6427	1.7261

3.2. Effects of applied voltage

The effect of the applied voltage on the refractive index of a given ionic liquid under three types of wavelengths (546 nm, 1013 nm, 1529 nm) are shown in Fig. 9. As seen for C_3MImI, the refractive index gradually decreases as the applied voltage increases. The refractive index of the working fluid C_3MImI decreases more slowly at the wavelengths of 546 nm and 1013 nm. The values of the C_3MImI refractive index at these two wavelengths under the conditions are very close to each other. However, the refractive index of C_3MImI and its derivative decrease with voltage at 1529 nm. The difference between the refractive indices of C_5MImI at the wavelengths of 546 nm and 1013 nm non-monotonically changes with the applied voltage (convex on the parabola), and the threshold voltage is about 0.75 V. When the anion is changed, the refractive index of the ionic liquid is also close to the values measured at the wavelengths of 546 nm and 1013 nm, but the refractive index first decreases and then increases with the applied voltage rising. In addition, when the anion is $[BF_4]^-$, the refractive index of the ionic liquid is more sencsitive to the change of the applied voltage, and the variation range is close to twice that when the anion is Br^-. In general, the test condition, *i.e.*, the effect of the wavelength of the light wave is the most basic, and the refractive indices measured at different wavelengths vary greatly (as in this case, from visible green light to infrared light). In addition, the influence of the carbon chain length of ionic liquid on the refractive index is very greatly equivalent to that of the anion species on the refractive index, which also provides an important reference for some electro–optic control designs.

For comparison, the effects of applied voltage on the refractive index of five types of ionic liquids are shown in Fig. 10. The relationships between the refractive index and voltage at a wavelength of 546 nm under the applied voltage for several ionic liquids are shown in Fig. 10(a), where Δn represents the change of the refractive index relative to the refractive index at the applied electric field of 0 V. When a voltage is applied to the ionic liquid at wavelength 546 nm, the refractive index does not change significantly. Comparatively, for three kinds of refrigerants, C_3MImI, C_4MImI, C_5MImI, their refractive indices decrease slightly with carbon chain length increasing. For a given long carbon chain, the refractive index first increases and then decreases gradually. The longer the carbon ring, the larger the increase degree is. When the number of carbon atoms is four, the variation of refractive index with applied voltage is smallest. Furthermore, when the anion is I^- and Br^-, the refractive index gradually increases with voltage increasing. When the anion is $[BF_4]^-$, the increase degree of the refractive index gradually decreases with applied voltage increasing.

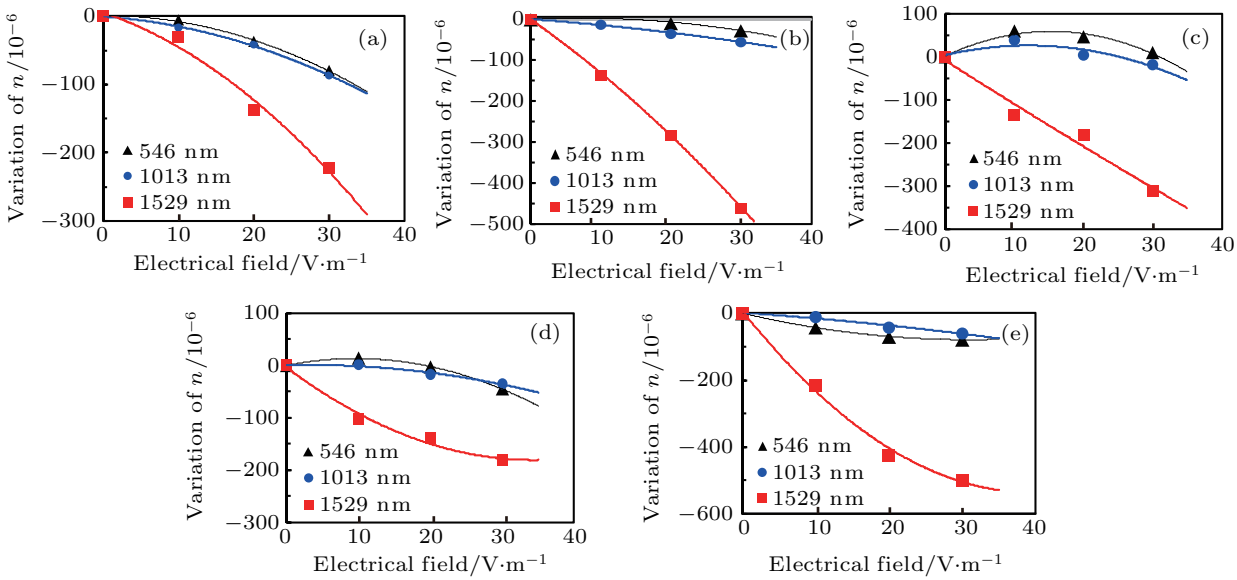

Fig. 9. Effects of applied voltage on refractive index for five types of ionic liquids: (a) C_3MImI, (b) C_4MImI, (c) C_5MImI, (d) C_3MImBr, and (e) C_4MImBF$_4$ at wavelengths of 546 nm, 1013 nm, and 1529 nm.

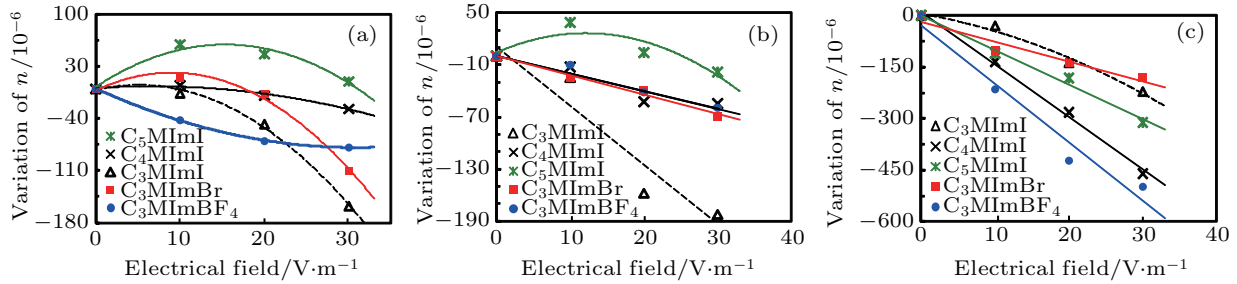

Fig. 10. Variations of refractive index with electric field for three types of ionic liquids at different wavelengths: (a) 546 nm, (b) 1013 nm, and (c) 1529 nm.

Effects of the applied voltage on the refractive index of three types of ionic liquids at the wavelength of 1013 nm are presented in Fig. 10(b). The three types of ionic liquids with different carbon chain lengths present different variation trends. The refractive index of C_5MImI first increases and then decreases with electric field increasing. The refractive index of C_4MImI tends to decrease slowly with electric field increasing, while the refractive index of C_3MImI decreases with electric field increasing. It can be concluded that when the number of carbon atoms in the carbon chain is greater than four, the refractive index tends to become larger as the applied electric field increases when the electric field is smaller. When the number of carbon atoms on the substituent decreases, this trend is no longer apparent, the refractive index becomes smaller as the electric field increases. In addition, the refractive index of C_3MImBr and C_3MImBF$_4$ decrease slowly with the increase of voltage, and the change of the refractive index of C_3MImBr is significantly smaller than that of C_3MImI with the applied electric field increasing.

The variations of refractive index of several ionic liquids with applied voltage at 1529 nm are shown in Fig. 10(c). With the increase of voltage, the refractive indices of five kinds of working media decrease, and their decreasing amplitudes at 1529 nm are larger than at 546 nm and 1013 nm. With the increase of carbon chain length, the refractive index changes with the applied electric field inceasing in the order of C_4MImI $>$ C_5MImI $>$ C_3MImI. The refractive index of C_4MImI and C_5MImI are almost the same, which are obviously smaller than that of C_3MImI. Because the size of cation and the length of alkyl chain may affect the refractive index of imidazolium salt, the contribution of the general polarizability of each CH_2 unit added to the chain is higher than that of the corresponding volume increase. It can be found that the change rule of refractive index with length of carbon chain is opposite to the change rule of absorption coefficient with voltage.[11] However, due to the change of anion, the refractive indices change with applied electric field in the order of C_3MImBF$_4$ $>$ C_3MImBr $>$ C_3MImI when the voltage is less than 1.0 V. The C_3MImBr belongs in weak current compared with C_3MImBF$_4$ for its weak oxidation of anion and is more difficult to polarize. At the same time, the initial refractive index of C_3MImI is largest at a given wavelength, but the change of refractive index is smallest when the electric field strength increases. In addition, when the voltage is small, the change of refractive index and absorption coefficient are opposite to each other under electric field.[11] Under the action of electric field, the change of absorption coefficient of the working medium with the increase of the change of refractive index decreases. In addition, com-

pared with the change of refractive index in the visible band, the effect of voltage on refractive index in the infrared band is significantly increased.

3.3. Discussion

From the experimental results, it can be seen that as the electric field increases, the refractive index as a whole tends to decrease and the absorption coefficient as a whole shows an increasing trend. Especially when the wavelength is close to 1520 nm, the above trend becomes more obvious. To this end, from the perspective of the evolution process of the ionic liquid anion and cation group, the response characteristics of the ionic liquid under the action of electric field and its effect on optical transmission performance are discussed.

As the external voltage increases, the evolution process can be divided into four phases, *i.e.*, electroneutrality, electric polarization, free carrier motion, and electrolysis.

(i) Electroneutrality phase

When the external voltage is zero, the anions and cations in the ionic liquid are connected through the ion bond and hydrogen bond. At this time, there is no change of macro concentration gradient in the liquid, the various ion clusters are randomly arranged in disorder, and they are electrically neutral.

(ii) Electric polarization phase

As the external voltage increases slowly, the electrode enters into the stage of electrode formation. At this time, the bond between anion and cation does not break under the action of electric field, forming a structure similar to electric dipole, and regular arrangement occurs along the direction of electric field under electric field.

(ii) Free carrier motion phase

When the applied voltage reaches a certain value, the ionic bond between anion and cation in the ionic liquid breaks and moves to the two electrode plates under the action of the applied electric field. Moreover, with the increase of voltage, the hydrogen bond between anion and cation in ionic liquid breaks, and the number of ionized anion and anion will increase gradually. At this time, it can be considered that the number of free carriers in ionic liquid is no longer stable, but increases with electric field strength increasing.

(iv) Electrolysis phase (breakdown)

When the applied electric field continues to increase and reaches to the electrochemical window value higher than that of the ionic liquid, the components of the ionic liquid will be separated. At this time, new chemicals will be separated from the left and right sides near the electrode, and the corresponding photorefractive properties will also change dramatically. In this study, the applied voltage is low and the discussion focuses on the first three stages, and the results are shown in Fig. 11.

Following the theory of polarization, the relative dielectric constant is a function of the electrode formation rate and satisfies formula (11), which includes the electrode formation rate,

$$\varepsilon_r = 1 + \chi e. \tag{11}$$

The refractive index and the dielectric coefficient satisfy

$$n = (\varepsilon_r \mu_r)^{1/2}. \tag{12}$$

Since the permeability values of most of the existing media are about equal to 1, the squared refractive index is roughly equal to the relative permittivity. It can be inferred from the two formulae that the polarizability and the refractive index increases with voltage incteasing.

The experimental results between 0 V and 0.5 V are in line with this trend, while other ionic liquids enter into the carrier motion phase at a voltage of 0.5 V because they cross the stage of polarization alignment. Therefore, its refractive index will gradually decrease.

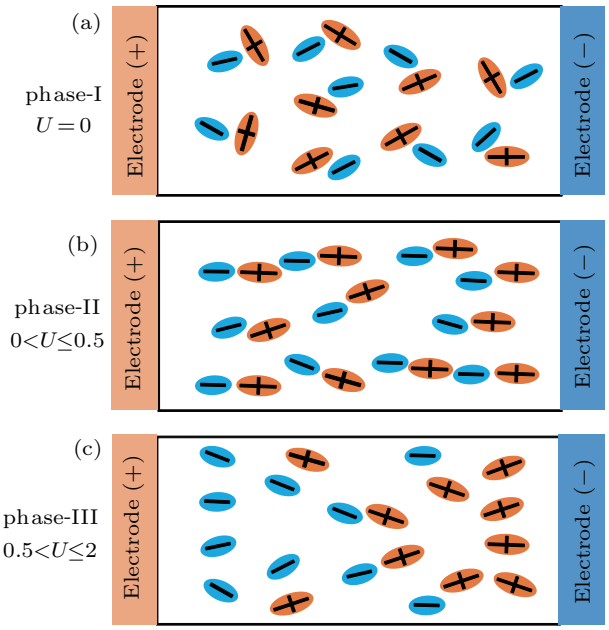

Fig. 11. Three typical phases of evolution process of ILs.

Referring to the relationship between the refractive index and the absorption coefficient and the carrier concentration in the above carrier transport theory, the electron concentration in the anion and the hole concentration in the cation at this time can be determined from the corresponding formulae. The change trend of the absorption coefficient increases, while the change trend of the refractive index decreases, which is consistent with the variation trend of the absorption coefficient and the refractive index when the voltage is increased to a certain extent. In addition, the absorption coefficient under the action of external electric field changes significantly with the applied electric voltage increasing. This can also be roughly compared with the result from Drude–Lorentz model[28,29] and

Kramers–Kronig model.[30,31] It can be seen from the equation that the change in absorption coefficient is related to the change of number of anions and cations, and the change of mobility of anion and cation. In addition, the denominators in Eq. (13) are squared, and the denominator in Eq. (14) is a single term, both of which can render the influence of carrier concentration change on the absorption coefficient greater.

$$\Delta\alpha = \frac{e^3\lambda_0^2}{4\pi^2c^3\varepsilon_0 n}\left[\frac{\Delta N_{\rm e}}{\mu_n\left(m_{\rm ce}^*\right)^2}+\frac{\Delta N_{\rm h}}{\mu_{\rm p}\left(m_{\rm ch}^*\right)^2}\right], \tag{13}$$

$$\Delta n = -\frac{q^2\lambda^2}{8\pi^2c^2n\varepsilon_0}\left(\frac{\Delta N_{\rm e}}{m_{\rm ce}^*}+\frac{\Delta N_{\rm h}}{m_{\rm ch}^*}\right). \tag{14}$$

As the movement of ions to the electrode plates at both ends is intensified, positive charges and negative charges with equal electric quantity gradually accumulate on the two electrode plates, and thus forming an internal electric field. The formation of the internal electric field will offset part of the external electric field, causing the ions to migrate to the two poles. The increase in resistance partially suppresses the tendency of the free carrier concentration increasing in the ionic liquid. Therefore, when the voltage increases to a certain value, the migration rate of anions and cations slow down, and the rate of change of the absorption coefficient and refractive index gradually decrease with voltage increasing.

Fundamentally, the refractive index is a measure of the dielectric response of a substance to an external electric field caused by electromagnetic waves. In the case of uniform and isotropic dielectrics, the response is governed by Lorentz–Lorenz equation:[32]

$$\frac{\alpha_{\rm e}}{\varepsilon_0} = 3\frac{M}{\rho N_A}\cdot\frac{n^2-1}{n^2+2}. \tag{15}$$

It can be seen from the above equation that when the ionic bond is broken as the polarization intensity increases, the refractive index decreases continuously. Since the polarization strength is proportional to the voltage across the two ends, The polarization strength increases in the form of an arithmetic progression in this experimental study. The refractive index is in the denominator and is a quadratic term. Therefore, the magnitude of the change in refractive index is much smaller than in electric field strength, which is consistent with the fact that the measured refractive index is less affected by the electric field.

4. Conclusions

In the present study, the light refraction properties of ionic liquids in a uniform electric field are investigated. A high precision hollow prism with electrodes on both sides is designed to measure the refractive index. An experimental program for measuring light refraction properties of ionic liquids in ultraviolet, visible, and near-infrared region is also developed. The laws for spectral refractive index varying electric field intensity of five kinds of imidazole ionic liquids are identified and illustrated. The hollow prism is determined by analyzing the system and the test error apex angle of minimum deviation error of machining accuracy. The propagated uncertainties involved in the measurement results are analyzed by using the uncertainty propagation formula for refractive index and determining the error range of the inversion results. The main conclusions drawn from the present study are as follows.

(I) The refractive index of the ionic liquid is reduced as the wavelength increases, the refractive indices of the five ionic liquids are in the order of C_3MImI $>$ C_4MImI $>$ C_5MImI $>$ C_3MImBr $>$ C_3MImBF_4; as the number of carbon atoms in the branch and anion and cation binding capacity (bond energy) increase, the refractive index of ionic liquid becomes gradually smaller.

(II) At the wavelength of 546 nm and 1013 nm, when the carbon chain grows, the refractive index first increases and then decreases with voltage increasing. The more the number of carbon chains, the more obvious the trend is. As the number of carbon chains decreases, the refractive index decreases. The voltage change does not increase first, but decreases all the time; as the wavelength becomes longer, the refractive index first increases and then decreases, and the refractive index decreases with voltage increasing. At a wavelength of 1529 nm, the refractive index decreases with voltage. The effect on the refractive index is less pronounced in the visible range than in other wavelength region.

(III) The variation trends of the refractive index and absorption coefficient are opposite to each other, and the variation range of refractive index is related to the polarization resistance. Under the action of electrical field, if an ionic liquid is easy to polarize, the refractive index of the ionic liquid is also quite easy to change. We also discover that when the refractive index of ionic liquid changes obviously with the electrical field, the absorption coefficient of that medium varies little with the electrical field. These results are consistent with the theory of electric polarization and carrier transport, and can be accounted for the dielectric properties of ionic liquid under the action of electric field.

The present study can provide the experimental means and data for further supporting the mechanism analysis and theoretical simulation of the electro–optical effect of ionic liquids, especially for the electro–optical regulation technologies used in the fields such as optical communication, optical sensing, optical displaying, high-power solid laser, smart glass, solar PV generation, *etc*. It also lays the foundation for further exploring the electro–optical regulation mechanisms and capabilities of ionic liquids, ionic liquid-like soft materials, and metamaterials.

References

[1] Nair J R, Colò F, Kazzazi A, Moreno M, Bresser D, Lin R, Bella F, Meligrana G, Fantini S, Simonetti E, Appetecchi G B, Passerini S and Gerbaldi C 2019 *J. Power Sources* **412** 398

[2] Hagiwara R and Ito Y 2000 *J. Fluor. Chem.* **105** 221

[3] Marsh K N, Boxall J A and Lichtenthaler R 2004 *Fluid Phase Equilib.* **219** 93

[4] Leighton C 2019 *Nat. Mater.* **18** 13

[5] Fan F R, Wu H, Nabok D, Hu S, Ren W, Draxl C and Stroppa A 2017 *J. Am. Chem. Soc.* **139** 12883

[6] Zhang C, Zhao W, Bi S, Rouleau C M, Fowlkes J D, Boldman W L, Gu G, Li Q, Feng G and Rack P D 2019 *ACS Appl. Mater. Interfaces* **11** 17979

[7] Dedzo G K and Detellier C 2018 *Adv. Funct. Mater.* **28** 1703845

[8] Lee K, Kim Y, Jung J, Ihee H and Park Y 2018 *Sci. Rep.* **8** 3064

[9] Xu F, Das S, Gong Y, Liu Q, Chien H C, Chiu H Y, Wu J and Hui R 2015 *Appl. Phys. Lett.* **106** 031109

[10] Wang F, Itkis M E, Bekyarova E and Haddon R C 2013 *Nat. Photon.* **7** 459

[11] Zhou J, Dong S K, He Z H, Caesar Puoza J L and Zhang Y H 2019 *Chin. Phys. B* **28** 017801

[12] Hayyan A, Mjalli F S, AlNashef I M, Al-Wahaibi Y M, Al-Wahaibi T and Hashim M A 2013 *J. Mol. Liq.* **178** 137

[13] Rilo E, Domínguez-Pérez M, Vila J, Segade L, García M, Varela L M and Cabeza O 2012 *J. Chem. Thermodyn.* **47** 219

[14] Wang X, Lu X, Zhou Q, Zhao Y, Li X and Zhang S 2017 *Phys. Chem. Chem. Phys.* **19** 19967

[15] Kang X, Zhao Y and Li J 2018 *J. Mol. Liq.* **250** 44

[16] Soriano A N, Ornedo-Ramos K F P, Muriel C A M, Adornado A P, Bungay V C and Li M H 2016 *J. Taiwan Inst. Chem. Eng.* **65** 83

[17] Chaudhary N and Nain A K 2018 *J. Mol. Liq.* **271** 501

[18] Zhang Q, Cai S, Zhang W, Lan Y and Zhang X 2017 *J. Mol. Liq.* **233** 471

[19] de Pablo L, Segovia Puras J J, Martín C and Bermejo M D 2018 *J. Chem. Eng. Data* **63** 1053

[20] Bhattacharjee A, Lopes-da-Silva J A, Freire M G, Coutinho J A P and Carvalho P J 2015 *Fluid Phase Equilib.* **400** 103

[21] Bhattacharjee A, Luís A, Santos J H, Lopes-da-Silva J A, Freire M G, Carvalho P J and Coutinho J A P 2014 *Fluid Phase Equilib.* **381** 36

[22] Seki S, Serizawa N, Ono S, Takei K, Hayamizu K, Tsuzuki S and Umebayashi Y 2019 *J. Chem. Eng. Data* **64** 433

[23] Zheng X, Gong Y, Jiang W, Yu K, Tong J and Yang J 2019 *J. Mol. Liq.* **288** 111004

[24] Shi R and Wang Y 2013 *J. Phys. Chem. B* **117** 5102

[25] Bai L, Li S N, Zhai Q G, Jiang Y C and Hu M C 2015 *Chem. Pap.* **69** 1378

[26] Montalbán M G, Bolívar C L, Díaz Baños F G and Víllora G 2015 *J. Chem. Eng. Data* **60** 1986

[27] Lide D R 1995 *CRC handbook of chemistry and physics* (Boca Raton: CRC Press) p. 382

[28] Paskov P P and Pavlov L I J A P B 1992 *Appl. Phys. B-Lasers Opt.* **54** 113

[29] Stagg B J and Charalampopoulos T T 1993 *Combust. Flame* **94** 381

[30] Peiponen K E and Vartiainen E M *Phys. Rev. B* **44** 8301

[31] Burba C M, Janzen J, Butson E D and Coltrain G L 2013 *J. Phys. Chem. B* **117** 8814

[32] Chiappe C, Margari P, Mezzetta A, Pomelli C S, Koutsoumpos S, Papamichael M, Giannios P and Moutzouris K 2017 *Phys. Chem. Chem. Phys.* **19** 8201